



## Pleiotropic effects of RecQ in *Deinococcus radiodurans*

Huan Chen<sup>a,b,1</sup>, Lifan Huang<sup>a,c,1</sup>, Xiaoting Hua<sup>a,1</sup>, Longfei Yin<sup>a,1</sup>, Yihuai Hu<sup>a,d,e</sup>, Chao Wang<sup>a</sup>, Weiwei Chen<sup>a</sup>, Xiaomin Yu<sup>f</sup>, Zhenjian Xu<sup>a</sup>, Bing Tian<sup>a</sup>, Songnian Hu<sup>f,\*</sup>, Yuejin Hua<sup>a,\*</sup>

<sup>a</sup> Key Laboratory for Nuclear-Agricultural Sciences of Chinese Ministry of Agriculture and Zhejiang Province, Institute of Nuclear-Agricultural Sciences, Zhejiang University, 310029, China

<sup>b</sup> Zhejiang Institute of Microbiology, Zhejiang Province, Hangzhou 310029, China

<sup>c</sup> Key Laboratory of Crop Genetics and Physiology of Jiangsu Province, Yangzhou University, 225009, China

<sup>d</sup> College of Life Sciences, Zhejiang University, Hangzhou 310029, China

<sup>e</sup> College of Life Sciences and Chemical Engineering, Huaiyin Institute of Technology, Huai'an 223001, China

<sup>f</sup> Key Laboratory of Genome Information and Sciences, Beijing Institute of Genomics, Chinese Academy of Sciences, Beijing 100029, China

### ARTICLE INFO

#### Article history:

Received 16 September 2008

Accepted 1 August 2009

Available online 10 August 2009

#### Keywords:

RecQ

*Deinococcus radiodurans*

Microarray

Reactive oxygen species

Manganese/iron

### ABSTRACT

In *Deinococcus radiodurans*, there is a unique RecQ homolog (DR1289) with three-tandem HRDC domains. Deletion of *drrecQ* resulted in a low doubling rate and sensitivity to hydrogen peroxide. Here, we used cDNA microarray and biochemical assays to explore the physiological changes in the *drrecQ* mutant. The expressions of genes with predicted functions involved in iron homeostasis, antioxidant system, electron transport, and energy metabolism were significantly altered in response to *drrecQ* disruption. More reactive oxygen species (ROS) was accumulated in *drrecQ* mutant strain when compared to wild type. In addition, ICP-MS results showed that the intracellular level of iron was relatively higher, whereas the concentration of manganese was lower in *drrecQ* mutant than in wild type. Furthermore, our microarray data and pulsed-field gel results showed that DNA suffered more damage in *drrecQ* mutant than in wild type under 20 mM hydrogen peroxide stress. These results suggested that *drrecQ* is a gene of pleiotropic functions and contributes to the extraordinary resistance of *D. radiodurans* against stresses.

Crown Copyright © 2009 Published by Elsevier Inc. All rights reserved.

### Background

The RecQ helicase homologues are highly conserved in evolution and are required for maintaining genome stability in all organisms [1]. RecQ helicases are characterized by their three conserved domains: the helicase domain, the RecQ C-terminal (RQC) domain, and the Helicase and RnaseD C-terminal (HRDC) domain [2]. All RecQ helicases that have been purified and characterized can unwind duplex DNA in a 3' to 5' direction with respect to the DNA strand bound by the helicase. The RecQ helicases are involved in various aspects of DNA metabolism, such as DNA replication, recombination repair, nonhomologous end-joining, telomere maintenance, and damage response [3,4].

Human RecQ homologues include BLM, WRN, and RECQL4, which are implicated in the human hereditary diseases Bloom's syndrome (BS), Werner's syndrome (WS), and Rothmund-Thomson syndrome (RTS), respectively. In particular, WS patients are predisposed to sarcomas and premature aging [5]. WRN plays a central role in the H<sub>2</sub>O<sub>2</sub>-induced cellular damage response pathway and the processing

of oxidative DNA lesions. Previous study has shown that oxidative lesions were not being efficiently detected and subsequently accumulated in WS cells [6]. Mutations of RecQ homologues in *Escherichia coli* (RecQ) and *Saccharomyces cerevisiae* (SGS1) resulted in an increased frequency of illegitimate recombination [7]. Sgs1 has been proposed as an important factor in S-phase checkpoint response of *S. cerevisiae*, where it may be both a 'sensor' for damage during replication and a 'resolvase' for irregular structures that arise at paused forks [8]. Deletion of SGS1 has demonstrated similar transcriptional responses to DNA damage and stress in yeast [9]. However, in prokaryotes, similar transcriptional response of the RecQ family has not yet been reported.

*Deinococcus radiodurans*, a bacterium famous for its extraordinary resistance to ionizing radiation, UV, desiccation, and a variety of DNA damaging agents [10], has a unique RecQ homologue (designated DrRecQ) with three tandem HRDC domains. Recently, Killoran and Keck [11] and our laboratory [12,13] have purified DrRecQ and characterized its biochemical function *in vitro*, confirming that DrRecQ possesses a remarkable ability to repair DNA damage in *D. radiodurans*. Recent research has shown that the DrRecQ null strain is extremely sensitive to H<sub>2</sub>O<sub>2</sub>, mitomycin C, UV, and gamma radiation [12–14]. To better elucidate the physiological functions of the unique DrrecQ protein, we monitored the transcriptome of the *drrecQ* mutant using cDNA microarray and other *in vitro* assays. The interesting effects of the *drrecQ* deletion on the physiological

\* Corresponding authors. S. Hu is to be contacted at fax: +86 01 82995401. Y. Hu, fax: +86 571 86971703.

E-mail addresses: [huan@big.ac.cn](mailto:huan@big.ac.cn) (S. Hu), [yjhua@zju.edu.cn](mailto:yjhua@zju.edu.cn) (Y. Hua).

<sup>1</sup> Huan Chen, Lifan Huang, Xiaoting Hua and Longfei Yin contributed equally to this work.

characteristics and gene expressions of *D. radiodurans* were observed and discussed.

## Results

### Growth features of the deletion mutant

By double crossover recombination, a *drrecQ* mutant (MQ) was generated by replacing the *recQ* gene with a kanamycin cassette. Compared to the wild type, aside from its higher sensitivity to DNA damage condition [13], compared to the wild type, the *drrecQ* mutant had a growth lag at the original stage of growth. To further confirm this result, we assayed the doubling time in lag phase and log phase. The *drrecQ* doubling time of  $3.47 \pm 1.6$  h was slightly slower than the  $1.56 \pm 0.19$  h doubling time of wild type under aerobic conditions in lag phase ( $p < 0.05$ ), but they did not show difference in log phase ( $P = 0.10$ ; Fig. 1).

### Transcriptional profiles of *drrecQ* mutant versus wild-type strain

To examine the expression of the entire gene repertoire of *D. radiodurans* in response to *recQ* knock-out simultaneously, the transcriptome of the *drrecQ* mutant was compared to that of wild type at exponential growth phase in normal growth conditions with cDNA microarray. We found that a total of 291 genes (about 9.1% of genome) showed at least a two-fold change, suggesting that these genes were affected by the deletion of the *drrecQ* gene through direct or indirect mechanisms. More genes were down-regulated than up-regulated (187 vs. 104). Based on COG database, we classified these 291 genes into 19 COG functional categories (Supplemental Table 1). The category with the most genes was the hypothetical proteins, which consists of genes that were both up- and down-regulated (51 and 71, respectively). Three categories in which genes were mostly repressed were E (amino acid transport and metabolism; 15), C (energy production and conversion; 16), and P (inorganic ion transport and metabolism; 23). All three down-regulated categories are associated with metabolism, which may be viewed as the cell's response to conserve energy and to minimize the generation of reactive oxygen species (ROS) [15].

Since the majority of the alterations in the transcriptome due to the deletion of *drrecQ* seems to be related to ROS emergency, we therefore mainly focused on the expression changes of four classes of genes encoding: (i) proteins with roles in anti-oxidative stress; (ii)

proteins with roles in DNA damage response genes; (iii) proteins with roles in iron metabolism; (iv) proteins associated with the production of ROS.

### Genes encoding proteins with roles in anti-oxidative stress

*D. radiodurans* possesses a powerful enzymatic antioxidant system, including catalases (DR1998, DRA0259, DRA0146), peroxidase (DRA0145), superoxide dismutases (Mn/Fe dependent: DR1279; Cu/Zn dependent: DR1546, DRA0202), and Dps proteins (DR2263, DRB0092) [10]. Several genes that are directly involved in ROS scavenging were strongly induced in response to *recQ* disruption, including three catalases (DR1998, 3.5-fold,  $p = 0.0000$ ; DRA0259, 1.9-fold,  $p = 0.0163$ ; DRA0146, 2.3-fold,  $p = 0.0000$ ), *sodC* (DRA0202, 2.6-fold,  $p = 0.0054$ ), and arginase (DRA0149, 2.2-fold,  $p = 0.0060$ ; Table 1). Furthermore, the gene expression levels of two Dps proteins, DR2263 and DRB0092, were decreased by two-fold ( $p = 0.0226$  and  $p = 0.0107$ ). Our recent results showed that DrOxyR (DR0615) is a repressor of DR2263 under oxidation stress [16]. For DRB0092, we found that it is negatively regulated by the DR2519 protein. DR2519 may be the homologue to DtxR in *Corynebacterium diphtheriae*, which has been shown to be a global transcriptional regulator of iron metabolism [17], or to MntR in *Bacillus subtilis*, which regulates the expression of two manganese transporters encoded by the *mntH* gene and the *mntABCD* operon [18] (our unpublished observation). In this study, DR2519 was slightly induced, and this may be a reason why DRB0092 was repressed.

### Genes encoding proteins with roles in DNA damage response

Three DNA damage response genes were induced, including *recA* (DR2340, 1.8-fold,  $p = 0.0168$ ), *recJ* (DR1126, 1.8-fold,  $p = 0.0106$ ), and *ddrM* (DR1440, 3.9-fold,  $p = 0.0000$ ) (Table 1). RecA is a major DNA repair protein, and a *recA* null strain is very sensitive to ionizing radiation when compared to wild type [19]. *ddrM* is induced under ionizing radiation, but its function is still unclear [19].

### Genes encoding proteins with roles in iron metabolism

Iron is an essential nutrient for all organisms, but it also poses problems of toxicity and poor solubility [20]. Like most bacteria, *D. radiodurans* has evolved various mechanisms to counter the iron toxicity and poor solubility, such as highly efficient iron acquisition systems and iron storage proteins [21]. Notably, in *drrecQ* mutant, almost all genes that are directly involved in iron transport were significantly repressed. These genes are involved in iron (III) transport system, hemin transport system, and ferrous iron transport system (Table 1). NADH dehydrogenase (DR1499), which is suggested to function as a ferric-reductase, was also repressed due to siderophore-mediated iron acquisition inhibition. This phenomenon indicated that *drrecQ* null mutant is under high-iron stress *in vivo*, and all the iron negative regulator, i.e., the Fe(II)-regulated genes are repressed, and genes specific for oxidative stress response are activated [22]. Expectably, we found the heme biosynthesis pathway (including HemB, HemD, HemE, HemH, HemG/Y, and HemN) was slightly induced. Hemes are biosynthesized from protoporphyrin and free ferrous iron and are cofactors for cytochromes, catalases and peroxidase. Indeed, DRA0259 (Fe-dependent catalase) and DRA0145 (Fe-dependent peroxidase) were also induced, both use heme as their cofactors.

### Genes encoding proteins associated with the production of ROS

Previous research showed that irradiated *D. radiodurans* strongly suppresses ROS produced by normal metabolism [23,24]. Generally, flavoproteins and cytochromes are regarded as the major sources generating such species within and outside of the respiratory chain [25,26]. In *drrecQ* mutant, three cytochromes (DR0434,  $-1.7$ -fold,  $p = 0.0002$ ; DRA0275,  $-1.77$ -fold,  $p = 0.055$ ; DRC0001,  $-2.22$ -fold,  $p = 0.0055$ ) and two flavoproteins (DR0970,  $-2.24$ -fold,  $p = 0.0068$ ;

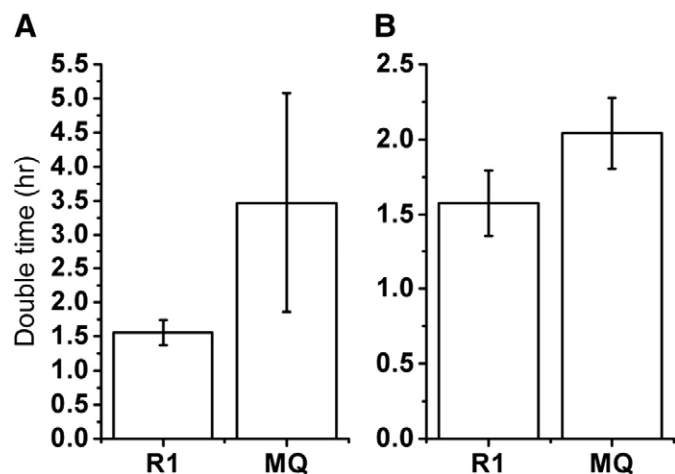


Fig. 1. Growth of wild-type *D. radiodurans* R1 compared to *drrecQ* mutant strains under normal condition in lag phase (A) and log phase (B). Error bars represent standard deviations from the averages of three biological replicate experiments. MQ: *recQ* mutant; R1: wild-type strain.

**Table 1**Wild-type strains under 20 mM H<sub>2</sub>O<sub>2</sub> stress compared to untreated *recQ* mutant.

| Classes                     | ORF     | Name            | Description                        | MQck<br>(log <sub>2</sub> -fold) | p value | R1H<br>(log <sub>2</sub> -fold) | p value |
|-----------------------------|---------|-----------------|------------------------------------|----------------------------------|---------|---------------------------------|---------|
| Anti-oxidative stress genes | DR1998  | <i>katE</i>     | catalase                           | 1.79                             | 0.0000  | 2.15                            | 0.0000  |
|                             | DRA0259 | <i>katE</i>     | catalase                           | 0.94                             | 0.0163  | 0.73                            | 0.0005  |
|                             | DRA0146 | <i>catA</i>     | catalase                           | 1.19                             | 0.0000  | 0.32                            | 0.0491  |
|                             | DRA0149 | <i>arginase</i> | polyamine biosynthesis             | 1.11                             | 0.0060  | 0.17                            | 0.2749  |
|                             | DRA0202 | <i>sodC</i>     | superoxide dismutases              | 1.37                             | 0.0054  | 0.11                            | 0.6449  |
|                             | DR2263  | <i>Dps</i>      | DNA protection during starvation   | −1.06                            | 0.0226  | −1.07                           | 0.0001  |
|                             | DRB0092 | <i>Dps</i>      | DNA protection during starvation   | −1.00                            | 0.0107  | −0.19                           | 0.2424  |
| DNA damage response genes   | DR1126  | <i>recJ</i>     | nuclease                           | 0.84                             | 0.0106  | −0.13                           | 0.5628  |
|                             | DR1440  | <i>ddrM</i>     | cation-transporting ATPase         | 1.98                             | 0.0000  | 0.15                            | 0.3562  |
|                             | DR2340  | <i>recA</i>     | recombinase                        | 0.84                             | 0.0168  | 1.04                            | 0.0039  |
| Iron metabolism genes       | DRB0014 | <i>hutB</i>     | hemin transport system             | −4.04                            | 0.0000  | 1.46                            | 0.0000  |
|                             | DRB0015 | <i>hutC</i>     | hemin-siderophore transport system | −1.79                            | 0.0034  | 0.17                            | 0.2793  |
|                             | DRB0016 | <i>hutD</i>     | hemin transport system             | −3.32                            | 0.0000  | 0.66                            | 0.0008  |
|                             | DRB0121 | <i>fhuC</i>     | iron (III) transport system        | −2.50                            | 0.0031  | 0.12                            | 0.5198  |
|                             | DRB0122 | <i>fecD</i>     | iron(III)-siderophore transport    | −2.50                            | 0.0003  | 0.10                            | 0.6495  |
|                             | DRB0123 | <i>fhuB</i>     | iron(III)-siderophore transport    | −2.52                            | 0.0009  | 0.12                            | 0.4537  |
|                             | DRB0125 | <i>Drb0125</i>  | iron transport system              | −5.82                            | 0.0000  | 1.32                            | 0.0000  |
|                             | DR1219  | <i>feoB</i>     | ferrous iron transport protein B   | −1.56                            | 0.0042  | 0.54                            | 0.0054  |
|                             | DR1220  | <i>feoA</i>     | ferrous iron transport protein A   | −1.78                            | 0.0000  | 0.26                            | 0.0861  |
|                             | DRB0017 | <i>drb0017</i>  | iron-chelator utilization protein  | −4.20                            | 0.0000  | 0.74                            | 0.0002  |
|                             | DRB0124 | <i>drb0124</i>  | iron-chelator utilization protein  | −4.68                            | 0.0000  | 0.80                            | 0.0030  |
|                             | DR0434  | <i>dr0434</i>   | cytochrome C6                      | −0.81                            | 0.0002  | 0.24                            | 0.1329  |
| ROS production genes        | DRA0275 | <i>dra0275</i>  | cytochrome C                       | −0.82                            | 0.0550  | −0.86                           | 0.0000  |
|                             | DRC0001 | <i>drc0001</i>  | cytochrome P450                    | −1.06                            | 0.0055  | −0.24                           | 0.1589  |
|                             | DR0970  | <i>fixB</i>     | oxidoreductase                     | −1.16                            | 0.0068  | 0.05                            | 0.7736  |
|                             | DR0971  | <i>fixA</i>     | flavoprotein subunit               | −1.26                            | 0.0026  | 0.15                            | 0.4302  |
|                             | DR1499  | <i>nqo3</i>     | NADH dehydrogenase subunit G       | −1.93                            | 0.0000  | 0.94                            | 0.0021  |
|                             | DR1506  | <i>nqo7</i>     | NADH dehydrogenase subunit A       | −1.40                            | 0.0002  | 0.54                            | 0.0061  |
|                             | DR2190  | <i>dr2190</i>   | NADH flavin oxidoreductase         | −1.63                            | 0.0000  | −0.44                           | 0.0244  |
|                             | DR1907  | <i>ykgE</i>     | Fe-S subunit of glycolate oxidase  | −1.61                            | 0.0007  | −1.14                           | 0.0000  |
|                             | DR1909  | <i>ykgF</i>     | Fe-S protein                       | −1.56                            | 0.0250  | −1.16                           | 0.0000  |

DR0971, −2.4-fold,  $p = 0.0026$ ) were significantly repressed. Furthermore, other three NADH-dependent enzymes included in respiratory chain were also inhibited (DR1499, −3.82-fold,  $p = 0.0000$ ; DR1506, −2.63-fold,  $p = 0.0002$ ; DR2190, −3.09-fold,  $p = 0.0000$ ; Table 1).

Finally, iron-sulphur proteins are dangerous under oxidation stress, not only because of the loss of Fe from iron-dependent enzymes will lead to the failure of the biochemical pathways in which they operate, but also because of the generation of HO<sup>•</sup> through the Fenton reaction (unbound Fe(II) reacting with H<sub>2</sub>O<sub>2</sub>) [25,27]. Expectedly, we observed a strong inhibition of three genes involved in iron-sulphur proteins family, including DR1499 (−3.82-fold,  $p = 0.0000$ ), DR1907 (−3.05-fold,  $p = 0.0007$ ), and DR1909 (−2.95-fold,  $p = 0.0250$ ).

#### Transcriptional profiles of *drrecQ* mutant under oxidative stress versus wild-type strain under normal condition

To determine how the *recQ* deletion affects the global transcriptional profile of *D. radiodurans* under oxidative stress, we also compared a global transcriptional profile of *drrecQ* mutant under H<sub>2</sub>O<sub>2</sub> treatment with that of wild type under normal condition. Through inspecting the expression profile of the *drrecQ* mutant strain, we found that a total of 208 genes were induced and 208 genes were repressed in response to H<sub>2</sub>O<sub>2</sub> stress. Supplemental Fig. 1 showed the classification of these genes according to COG database. Among the 208 up-regulated genes, 16 genes were found in wild-type strain under hydrogen peroxide stress and 73 genes were induced because of the *drrecQ* deletion (Supplemental Fig. 2A). The top four categories with the most genes were HP (hypothetical protein; 85), R (general function prediction only; 19), S (function unknown; 17), and L (DNA replication, recombination and replication; 16). Meanwhile, of the 208 down-regulated genes, 12 genes were repressed in wild type under hydrogen peroxide stress and 59 genes were

inhibited caused by the mutation of *drrecQ* (Supplemental Fig. 2B). The largest repressed groups were again the hypothetical proteins (65), J (Translation, ribosomal structure and biogenesis; 34), E (Amino acid transport and metabolism; 20), and I (Lipid metabolism; 11). Among 50 ribosomal proteins in *D. radiodurans* genome, 41 proteins were strongly repressed. These observations were consistent with the fact that 20 mM H<sub>2</sub>O<sub>2</sub> was a fatal dose to the *drrecQ* mutant.

To better compare to the transcriptional profiles of *drrecQ* mutant versus wild-type strain under normal condition, we also focused on the expression patterns of the same four gene classes described previously.

#### Genes encoding proteins with roles in anti-oxidative stress

Compared to mutant under normal growth condition, both the number of oxidation stress response-related genes and their expression levels showed an obvious increase under 20 mM H<sub>2</sub>O<sub>2</sub> (Table 2). For example, *msrA* (DR1849, 4.5-fold,  $p = 0.020$ ), which repairs oxidized proteins through the reduction of the protein-bound methionine sulfoxide back to methionine via a thioredoxin-recycling process, was activated. Another gene, *grxA*, which encodes for glutaredoxin, was induced by 3.3-fold ( $p = 0.0078$ ). Under oxidative stress, glutaredoxin catalyzes the reduction of disulfide bonds in proteins, converting glutathione to glutathione disulfide, and restores the proteins' activities [27].

#### Genes encoding proteins with roles in DNA damage response genes

Similar to anti-oxidative genes, there were more DNA repair genes induced, e.g. *recA*, *recD*, *pprA*, *ddrA*, *uvrA*, *sbcD* and *uvrD*. Moreover, some uncharacterized genes were also highly induced, such as *ddrB* (DR0070), which was up-regulated by 22.4-fold ( $p = 0.0007$ ), and *ddrC*'s expression (DR0003) was increased by 15.1-fold ( $p = 0.0013$ ). Previous studies showed that *ddrB* mutant was more sensitive to acute irradiation than wild-type R1 [19]. This suggested that the genome was damaged and double-stranded breaks (DSBs) were

**Table 2**Wild-type strains 20 mM H<sub>2</sub>O<sub>2</sub> stress compared to *recQ* mutant under 20 mM H<sub>2</sub>O<sub>2</sub> stress.

| Classes                     | ORF     | Name           | Description                                 | MQH (fold) | p value | R1H (fold) | p value |
|-----------------------------|---------|----------------|---|------------|---------|------------|---------|
| Anti-oxidative stress genes | DR1998  | <i>katE</i>    | catalase                                    | 2.77       | 0.0004  | 2.15       | 0.0000  |
|                             | DRA0259 | <i>katE</i>    | catalase                                    | 1          | 0.1114  | 0.73       | 0.0005  |
|                             | DRA0146 | <i>catA</i>    | catalase                                    | 1.20       | 0.0125  | 0.32       | 0.0491  |
|                             | DRA0202 | <i>sodC</i>    | superoxide dismutases                       | 1.49       | 0.0199  | 0.11       | 0.6449  |
|                             | DR1857  | <i>osmC</i>    | alkylperoxide and oxidative stress response | 0.95       | 0.1045  | 1.20       | 0.0000  |
|                             | DR1849  | <i>msrA</i>    | peptide methionine sulfoxide reductase      | 2.16       | 0.0205  | 0.08       | 0.5805  |
|                             | DR2085  | <i>grxA</i>    | glutaredoxin                                | 1.71       | 0.0078  | −0.71      | 0.0007  |
|                             | DR1775  | <i>uvrD</i>    | helicase II                                 | 1.32       | 0.0080  | 0.14       | 0.4717  |
| DNA damage response genes   | DR1902  | <i>recD</i>    | helicase/exonuclease                        | 3.02       | 0.0019  | 0.13       | 0.3953  |
|                             | DR1921  | <i>sbcD</i>    | exonuclease                                 | 1          | 0.0236  | 0.58       | 0.0022  |
|                             | DR1922  | <i>sbcC</i>    | exonuclease subunit, predicted ATPase       | 1.05       | 0.0092  | 0.32       | 0.0466  |
|                             | DR2275  | <i>uvrB</i>    | helicase                                    | 2          | 0.0120  | 0.48       | 0.0663  |
|                             | DR2340  | <i>recA</i>    | recombinase                                 | 2.72       | 0.0145  | 1.04       | 0.0039  |
|                             | DR2438  | <i>Nth</i>     | endonuclease III and thymine glycol         | 1.89       | 0.0142  | −0.58      | 0.0027  |
|                             |         |                | DNA glycosylase                             |            |         |            |         |
|                             | DRA0188 | <i>uvrA</i>    | ATPase, DNA binding                         | 1.15       | 0.1082  | −0.12      | 0.4517  |
|                             | DRA0346 | <i>pprA</i>    | DNA damage repair protein                   | 3.17       | 0.0703  | 0.52       | 0.0341  |
|                             | DR0003  | <i>ddrC</i>    | predicted protein                           | 3.92       | 0.0013  | −0.24      | 0.1437  |
|                             | DR0070  | <i>ddrB</i>    | predicted protein                           | 4.49       | 0.0007  | 0.54       | 0.0047  |
|                             | DR0219  | <i>ddrF</i>    | predicted protein                           | 1.71       | 0.0120  | 0.12       | 0.4907  |
|                             | DR0326  | <i>ddrD</i>    | predicted protein                           | 2.53       | 0.0004  | 0.03       | 0.8431  |
|                             | DR0421  | <i>dr0421</i>  | predicted protein                           | 1.49       | 0.0749  | −0.42      | 0.0336  |
|                             | DR0438  | <i>ddrH</i>    | predicted protein                           | 1.21       | 0.0415  | −0.23      | 0.1191  |
|                             | DR0659  | <i>frnE</i>    | predicted protein                           | 1.05       | 0.0593  | −0.31      | 0.0547  |
|                             | DR1440  | <i>ddrM</i>    | cation-transporting atpase                  | 2.07       | 0.0708  | 0.15       | 0.3562  |
|                             | DR2441  | <i>ddrN</i>    | NH <sub>2</sub> -acetyltransferase          | 2.44       | 0.0010  | 0.10       | 0.5223  |
|                             | DR2574  | <i>ddrO</i>    | HTH transcription factor, phage type        | 2.10       | 0.0126  | 1.20       | 0.0001  |
|                             | DRB0017 | <i>drb0017</i> | iron-chelator utilization protein           | −1.03      | 0.0785  | 0.74       | 0.0002  |
|                             | DR1131  | <i>hemZ</i>    | ferrochelatase                              | 0.95       | 0.0481  | 0.19       | 0.1672  |
|                             | DR1502  | <i>dr1502</i>  | NADH dehydrogenase subunit                  | −1.04      | 0.3540  | 0.81       | 0.0008  |
|                             | DR1506  | <i>nqo7</i>    | NADH dehydrogenase subunit                  | −1         | 0.0687  | 0.54       | 0.0061  |
|                             | DR1907  | <i>ykgE</i>    | Fe-S subunit of glycolate oxidase           | −2.51      | 0.0031  | −1.14      | 0.0000  |
|                             | DR1909  | <i>ykgF</i>    | Fe-S protein                                | −2.12      | 0.0155  | −1.16      | 0.0000  |
| Iron metabolism genes       |         |                |   |            |         |            |         |
| ROS production genes        |         |                |   |            |         |            |         |

generated after *drrecQ* mutant strain underwent 20 mM hydrogen peroxide stress.

#### Genes encoding proteins with roles in iron metabolism

The most down-regulated gene in this class was DRB0017, which is an iron-chelator utilization protein. Other iron transport genes were slightly repressed. Another significantly changed gene was *hemZ* (DR1131, 2-fold,  $p = 0.0481$ ), and it is involved in heme biosynthesis.

#### Genes encoding proteins associated with the production of ROS

We still found four genes being inhibited. Among them, two belonged to the respiratory chain (DR1502 and DR1506), and the other two were Fe-S proteins (DR1907 and DR1909).

#### Verification of gene expression level changes by real-time quantitative PCR and Western blot

Five genes were examined further for their expression level changes by real-time PCR assay using the same experimental growth conditions as applied for the microarray analyses. They were *recA* (DR2340), *katE* (DR1998), *dps* (DR2263), *minD* (DR2383), and *minE* (DR0751) (Fig. 2B). DrRecA protein is an essential factor for extreme radiation resistance. This protein is normally expressed at a very low level in *D. radiodurans* and at a high level after heavy DNA damage [23]. Real-time PCR showed that *recA* levels increased by 1.6-fold in response to *recQ* deletion and increased by 16.7-fold in *drrecQ* mutant after 20 mM H<sub>2</sub>O<sub>2</sub> damage. The expression pattern is the same as the microarray data (Fig. 2A).

We further investigated the protein expression level changes of DrRecA in the wild-type R1 strain and in the *drrecQ* mutant, with or without the 20 mM H<sub>2</sub>O<sub>2</sub> treatment. As shown in Fig. 2C, Western blot results showed that the expression level of RecA was 2.7-fold higher than that of R1 in the *drrecQ* deletion strain and was 3.0-fold higher

than that of R1 undergoing 20 mM H<sub>2</sub>O<sub>2</sub>. Although the changes in transcription and translation are not equal, the increased expression of DrRecA in *drrecQ* mutant in normal condition and under stress are of the same trend.

*dr1998* encodes for KatE, a major catalase in *D. radiodurans*, and it has been shown to play a role in protection of *D. radiodurans* from oxidative stress and ionizing radiation [28]. *dr2263* is a *dps* gene, with functions of protection against oxidative stress and iron uptake and storage [29,30]. Our previous study showed that *katE* is positively regulated by OxyR, while *dps* (*dr2263*) is negatively controlled by OxyR under oxidation stress [16]. Both of the expression patterns of these two genes showed that deletion of *recQ* would increase sensitivity of cell to oxidant stress. When the *drrecQ* mutant was treated with 20 mM H<sub>2</sub>O<sub>2</sub>, as well as wild-type strain under ionizing radiation [23,24], *dps* is highly induced, suggesting that DNA was seriously damaged.

Due to the slower doubling rate of the mutant strain than wild type, the expression levels of two Min family proteins, MinD and MinE, which were known to regulate cell division, were measured (Fig. 2B). Interestingly, we found *minD*, a cell division inhibitor, was induced in all three conditions (wild type under H<sub>2</sub>O<sub>2</sub> stress, *recQ* disruption, and *recQ* disruption under H<sub>2</sub>O<sub>2</sub> stress), whereas *minE*, which is a factor that can prevent division inhibitor from acting at internal division sites, was inhibited in these three conditions.

#### Defect in RecQ causes ROS accumulating in *drrecQ* mutant

Since the three top repressed categories were all involved in metabolism (Supplemental Table 1), and many anti-oxidant genes were induced (Table 1), it could be inferred that ROS were accumulated in *drrecQ* mutant. To test this hypothesis, we assayed the ROS concentration in wild-type strain and in *drrecQ* mutant in log phase, either under H<sub>2</sub>O<sub>2</sub> (20 mM) treatment or not. Compared under the



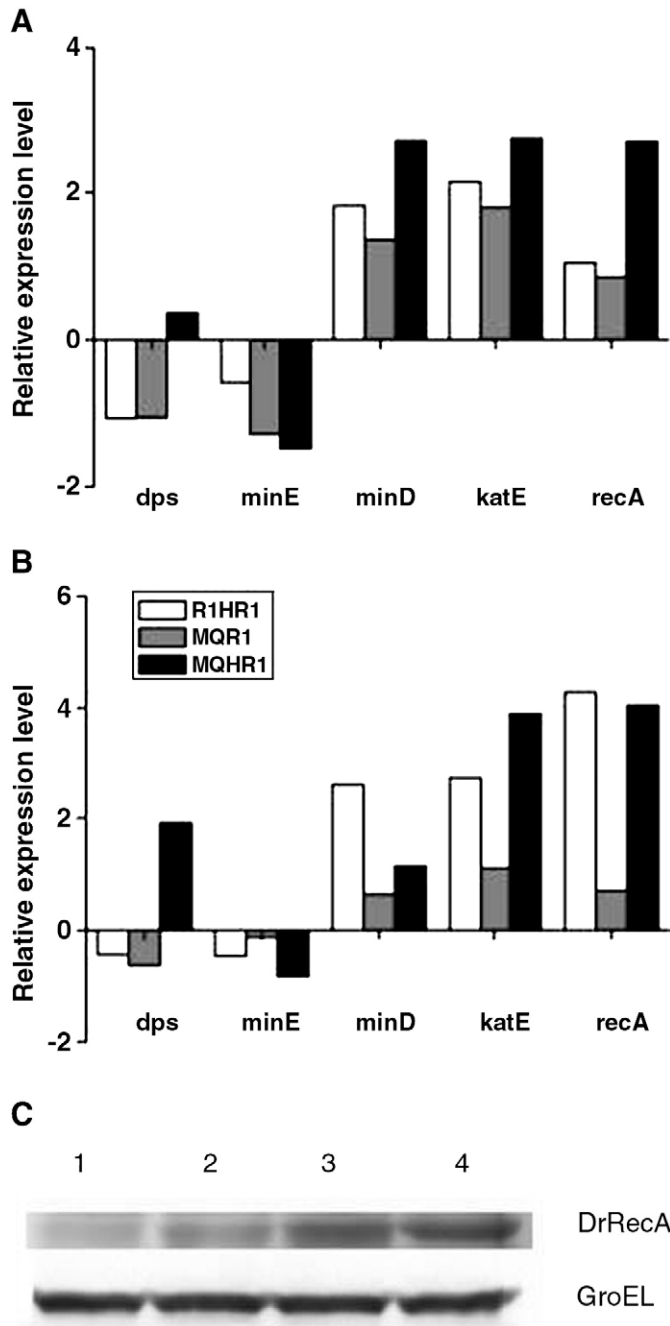


**Fig. 2.** Verification of gene expression changes with real-time quantitative PCR and Western blot. Five genes were selected and their expression patterns from the microarray data (A) were compared to those with real-time quantitative PCRs (B). The results showed that their expression patterns were highly correlated. R1HR1: wild-type strains treated with 20 mM  $H_2O_2$  for 30 min compared to untreated wild-type strain; MQR1: untreated *recQ* mutant compared to untreated wild-type strains; MQHR1: *recQ* mutant treated with 20 mM  $H_2O_2$  for 30 min compared to untreated wild-type strains. (C) Changes in intracellular RecA protein levels of wild-type strains and *drrecQ* mutant strains under normal condition and  $H_2O_2$  stress condition (20 mM), respectively. Band 1 is wild-type under normal condition, Band 2 is wild-type under  $H_2O_2$  stress condition, Band 3 is *drrecQ* mutant strains under normal condition, and Band 4 is *drrecQ* mutant strains under  $H_2O_2$  stress condition. GroEL was used as a loading control.

same phase of normal growth, we determined the ROS concentration in *drrecQ* mutant was higher than in wild-type strain ( $p = 0.037$ ) (Fig. 3). Similarly, when exposed to  $H_2O_2$ , *drrecQ* mutant accumulated more ROS concentration than wild-type strain ( $p = 0.107$ ), although the ROS concentration was significantly higher than those under normal growth (Fig. 3).

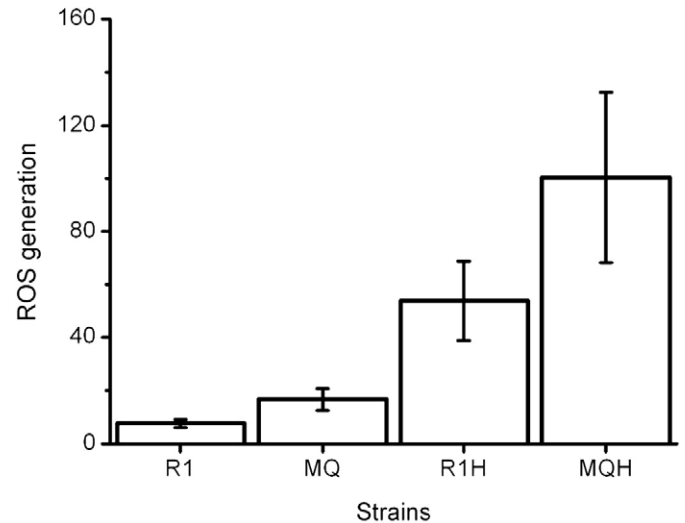


**Fig. 3.** ROS generation in wild-type strain and *recQ* mutant with or without 20 mM hydrogen peroxide exposure. Data reported represent the average and standard error of the mean of three independent experiments. R1: wild-type strains under normal condition; R1H: wild-type strains treated with 20 mM  $H_2O_2$ ; MQ: *recQ* mutant under normal condition; MQH: *recQ* mutant treated with 20 mM  $H_2O_2$ .

#### Defect in RecQ causes low Mn/Fe in *drrecQ* mutant

Because many iron-dependent transport proteins were strongly repressed in *drrecQ* mutant from our microarray data, we monitored the intercellular level of iron in different strains by inductively coupled plasma-optical emission spectroscopy (ICP-MS). As shown in Table 3, the iron and manganese ions concentrations were altered in *drrecQ* mutant. Compared to levels of Mn and Fe in wild-type R1, *drrecQ* mutant had less Mn and more Fe, leading to the decrease of the ratio of Mn:Fe (Mn/Fe) from 0.38 to 0.07. Previous work proposed that high intracellular Mn/Fe of *D. radiodurans* might underline the efficiency of its repair pathways by protecting cells from ROS generated during recovery [31]. According to this hypothesis, a decrease of Mn/Fe might increase ROS production. Under these severe circumstances, cells would activate anti-oxidation mechanisms to lower free ferrous iron and scavenge ROS. Otherwise, the expression level of Mn-dependent transport systems (DR1709) would be induced in response to low cellular Mn concentration. Interestingly, the electron paramagnetic resonance (EPR) assay results showed that the mutant accumulated approximately two times less intracellular ‘free’ iron ions than wild type (Fig. 4). It might be resulted from the block of iron transport systems.

#### Discussion

Extensive studies in the *D. radiodurans* have revealed several related recovery mechanisms, and DNA repair mechanism is the most important one. Among DNA repair proteins, RecQ is unusual among

**Table 3**  
Intracellular Mn and Fe levels.

| Strains      | Total Mn (nmol Mn/ $10^8$ cell) | Total Fe (nmol Fe/ $10^8$ cell) | Intracellular Mn/Fe concentration ratio |
|--------------|---------------------------------|---------------------------------|---|
| R1-CK        | $1.05 \pm 0.24$                 | $2.77 \pm 1.08$                 | 0.38                                    |
| R1- $H_2O_2$ | $1.49 \pm 0.15$                 | $3.06 \pm 0.44$                 | 0.49                                    |
| MQ-CK        | $0.46 \pm 0.12$                 | $7.05 \pm 2.77$                 | 0.07                                    |
| MQ- $H_2O_2$ | $0.55 \pm 0.05$                 | $9.03 \pm 1.69$                 | 0.06                                    |

Strains were grown to OD600 0.3 in TGY medium. The samples were treated as previously and subjected to ICP-MS [31,33].

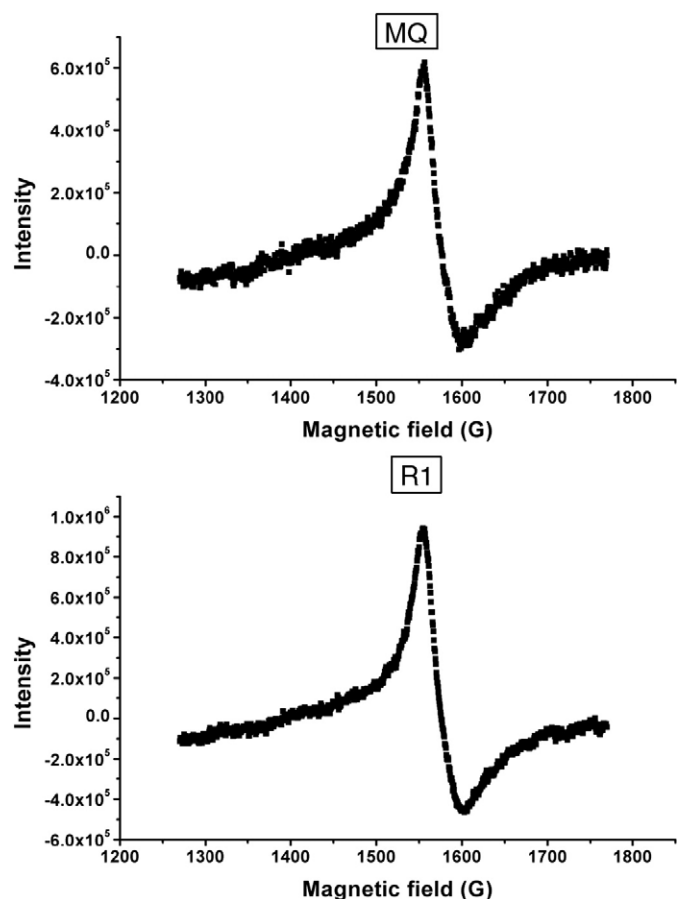


**Fig. 4.** EPR signal of iron from whole-cell preparations. Both wild-type strain (R1) and *recQ* mutant cell densities were adjusted to equal before filling in the quartz EPR tubes according to measured OD600 value of each strain. The major signal appears at  $g = 4.3$ . Average values of triplicate experiments are shown. R1: wild-type strains; MQ: *recQ* mutant.

RecQ family members in that it has evolved to utilize three 'Helicase and RnaseD C-terminal' domains to carry out its activity [11–13]. In this study, multiple effects of *drrecQ* on the *D. radiodurans* transcriptome were demonstrated by cDNA microarray technology together with biochemical assay.

The response of *D. radiodurans* to the disruption of *recQ* was characterized, most notably, with the induction of genes with annotated functions in iron metabolism, cell cycle, oxidative-related genes, as well as amino acid transport, and metabolism. *drrecQ* deletion mutant showed a similar phenotype to wild type under oxidative stress. This expression pattern is same as the *sgs1* mutant profile under normal condition, both mutations are seen as under cellular damage and stress even when grown under theoretically nonharmful conditions [9]. As expected, we found that the *drrecQ* mutant accumulated more ROS than the wild-type strain. Furthermore, pulsed-field gel was used to detect whether there are obvious DSBs production in the mutant genome. The results showed that DSBs were not produced obviously in the *drrecQ* mutant (MQ) genome under normal growth condition, as well as in wild-type strain genome under 20 mM  $H_2O_2$  stress (Supplemental Fig. 3). Based on these characteristics, we proposed that the level of ROS production in the mutant could not be causing a lot of DSBs, and single-strand damaged DNA and DNA adducts might be the major products, for genes involved in NER (*uvrA* and *uvrD*) are induced.

An interesting finding in this study was that Fe and Mn metabolism was affected by *drrecQ* deletion. Some phenotypes of *drrecQ* mutant were very similar to the SO1377 knock-out mutant

in *Shewanella oneidensis* MR-1 [32]. Both mutants showed an anti-oxidative phenomenon and a lower free iron concentration compared to wild type. However, *drrecQ* mutant accumulated more total iron than wild type did, but the total intracellular iron was not changed in SO1377 mutant and its wild type. Deletion of *drrecQ* caused an increased total iron concentration and higher ROS level. ROS could damage proteins, especially those containing iron–sulphur clusters or sulphur atoms and DNA (caused by Fenton-type chemistry) [33,34]. To combat the oxygen stress, cells activate some pathways to reduce the concentration of free iron, which could mediate the production of highly toxic hydroxyl radical. Firstly, Fe-dependent transport systems in MQ were significantly repressed by an induction of transcriptional regulator(s) of iron repressor, for which ionic Fe (II) is used as a co-repressor; secondly, we found the heme biosynthesis pathway (including HemB, HemD, HemE, HemH, HemG/Y, HemN) was slightly induced. Finally, some iron binding proteins raised their expression levels to bind free iron, such as ferredoxin (DR2330). Consequently, consistent with EPR results, the concentration of 'free' iron ions was decreased.

In addition, the level of Mn ions was reduced in *drrecQ* mutants. Mn is required for the growth and survival of most living organisms, and the critical role of Mn homeostasis in bacteria has been proven [35]. High intracellular Mn(II) concentrations are known to efficiently scavenge  $O_2^-$  and hold DNA that contains several single-strand breaks together, and Mn(II) does not participate in Fenton-type chemistry [31]. More recent research showed that protein oxidation was implicated as the primary determinant of *D. radiodurans* radio-resistance, and Mn accumulation in *D. radiodurans* could prevent protein from oxidation [36]. The low concentration of Mn(II) caused by *drrecQ* deletion was not sufficient to stabilize opposed DNA single-strand breaks and decreased the protective ability on protein during oxidative stress.

This study provides the first global view of the transcriptome alteration in the *drrecQ* mutant. Taken together, we proposed that *drrecQ* deletion would cause ROS accumulation and Fe and Mn metabolism alterations. This may be a new way to explain why *drrecQ* mutant is so vulnerable to  $H_2O_2$ . In eukaryotic cells, cumulative oxidative damage has been implicated in a number of disease states such as cancer and the aging process, and previous research also showed that *recQ* mutant would result in genetic disorders and premature aging. Our results suggest that mutation of *recQ* would lead to cumulation of oxidative damage, and might lead to the aging process.

## Material and Methods

### Bacterial strains and growth conditions

The bacterial strain *D. radiodurans* R1 and *drrecQ* mutant strain [14] were cultured at 30 °C in TGY media (0.5% Bacto tryptone, 0.1% glucose, 0.3% Bacto yeast extract) with aeration, or on TGY plates supplemented with 1.3% agar. All cells in this article were grown to mid-log phase ( $OD_{600}$  0.2–0.3). Cells were harvested by centrifugation at 5000 g at 4 °C, washed three times with PBS, and quickly frozen for storage at –80 °C.

### Doubling time measurement

Growth measurement was done as described previous [37]. Briefly, 500  $\mu$ l overnight culture of each strain was transferred to 50 ml TGY. The cultures were grown at 30 °C at 200 rpm. The dilutions were spread onto TGY agar plates after 2 h ( $t_1$ ) and 4 h ( $t_2$ ). The plates were incubated at 30 °C for 5 days, and the number of colony-forming units (CFU) was determined. The doubling time,  $g$ , was calculated from the equation  $g = \ln 2 / [(\log_{10} N_2 - \log_{10} N_1) 2.303 / \Delta t]$ , where  $N_1$  is CFU per milliliter at  $t_1$ , and  $N_2$  is CFU per milliliter at  $t_2$ .

### RNA isolation, probe preparation, microarray hybridization and data analysis

Total RNA was extracted from 50 mL of cultures of *D. radiodurans* using TRIZOL Reagent (Invitrogen Corp., Carlsbad, CA) following liquid nitrogen grinding. Then, the RNA sample from each condition was treated with 10 units of RNase free DNase I (Promega, Mannheim, Germany) and purified using phenol–chloroform extraction. RNA quality and quantity were evaluated by UV absorbance at 260 and 280 nm.

Microarray fabrication and hybridization were prepared as published [24]. Briefly, 2996 pairs of gene-specific PCR primers were designed by PRIMEGENS software [38], and 100 pairs were designed by Primer3. All primers were screened through Blastn. In total, 3096 pairs of primers were synthesized. PCR products were generated and purified, yielding a collection of 3084 distinct ORFs (single band and >100 ng/μl). Each ORF was printed twice on each array. Because of high variability in microarray hybridization, two replicated samples were obtained, and the RNA obtained from each sample was hybridized with dye-swap. Thus, eight data points were available for each experiment.

GenePix pro 5.1 was used to quantify the hybridization signals. Normalization and statistical analysis were carried out in the R computing environment using the linear models for microarray data package (Limma) [39]. Prior to channel normalization, microarray outputs were filtered to remove spots of poor signal quality by excluding those data points with a mean intensity less than two standard deviations above background in both channels. Within Limma global LOESS normalization was carried out for each microarray [40], and the within-array correlation method was used to average the replicate spots [41]. In this study there were three parallel experiments: (i) untreated wild-type strains compared to wild-type strains treated with 20 mM H<sub>2</sub>O<sub>2</sub> for 30 min, (ii) untreated wild-type strains compared to untreated *recQ* mutant, and (iii) untreated wild-type strains compared to *recQ* mutant treated with 20 mM H<sub>2</sub>O<sub>2</sub> for 30 min. For each experiment, three independent cell cultures were performed and used as biological replications. All microarray data was supplied in Supplemental Table 3.

### Real-time quantitative PCR

Eight genes were picked out for real-time quantitative PCR. Among them, DR0089, a gene whose expression is unaffected by H<sub>2</sub>O<sub>2</sub> and ionizing radiation, was regarded as a normalization factor. Other information was described in Supplemental Table 2 and Supplemental Fig. 1 in detail. In short, first-strand cDNA synthesis was carried out in 20 μl of reactions, containing 1 μg of each DNase I-treated and purified total RNA sample, combined with 3 μg of random hexamers. The real-time PCR amplification used Quant SYBR Green PCR (TIANGEN BIOTECH Co., Ltd. USA) following the manufacturer's instructions. All assays were performed using the iCycler iQTM real-time detection system (Bio-Rad, Hercules, CA).

### Assay of intracellular ROS accumulation

ROS generation in cells was assayed as published [42]. Briefly, 1 mL of DCFH-DA (10 μM) was added to cells (2000 μL, OD<sub>600</sub> = 0.3, washed three times with PBS) and incubated at 37 °C for 20 min with slight shaking. After incubation, the cells were washed twice with PBS and resuspended in 200 μL PBS. The sample was then divided in half, half of the culture (100 μL) was exposed to 1 μL H<sub>2</sub>O<sub>2</sub> (1 M) for 20 min at room temperature, the nonexposed control culture was incubated concomitantly. The fluorescence intensities were measured using a fluorescence spectrophotometer with an excitation wavelength of 485 nm and an emission wavelength of 525 nm. Cell numbers were determined by plate assay.

### Western blot analysis

The cells were lysed by sonication on ice at 500 W output for a total of 5 min and the debris were removed by centrifugation (20,000 × g, 30 min). Soluble lysate was analyzed by SDS-PAGE, and proteins were detected with DrRecA antibody (rabbit IgG, laboratory stock). The protein concentration was determined by the Bradford method with BSA as the standard.

### Assay of intracellular iron and manganese concentration

Total Fe and Mn concentration were detected as described previously with some modification [33]. Bacteria were grown aerobically to OD<sub>600</sub> 0.25 in 400 mL of TGY broth. After centrifugation at 10,000 × g for 10 min at 4 °C, cells were washed twice in 200 mL of PBS with 1 mM EDTA (pH 7.4) and resuspended in 200 mL of PBS without EDTA. After centrifugation, the pellet was resuspended in 10 mL of PBS. For iron analysis, pelleted bacteria were resuspended in 1 mL of Ultrex II nitric acid (Fluka AG, Buchs, Switzerland) and incubated at 80 °C for 1 h. After centrifugation at 20,000 × g for 20 min, the supernatant was filtered against 0.45-μm membrane. The concentration of samples was analyzed for Fe and Mn content by ICP-MS (Model Agilent 7500a, Hewlett-Packard, Yokogawa Analytical Systems, Tokyo, Japan). The determination of Fe was based on Iron 57 Metal Isotope. All buffers and nitric acid solutions were analyzed as described above to correct for background.

### Assay for whole cell EPR spectroscopy

The procedure for EPR assay was adapted from Keyer and Imlay [43]. After 24 h of growth with shaking in 200 mL TGY liquid at 30 °C, the optical density (OD<sub>600</sub>) of the culture was measured. Cells were spun down at room temperature and suspended in fresh 50 mL TGY liquid containing 20 mM desferrioxamine (DFO) (Sigma Chemical, Deisenhofen, Germany). After incubation with shaking for 20 min at 30 °C, cells were spun down, washed with cold 20 mM Tris (pH 7.4), resuspended in 20 mM Tris (pH 7.4) containing 10% glycerol to reach the same cell density according to OD<sub>600</sub> value measured, frozen in 3-mm quartz EPR tubes (Wilma Glass Co., Buena, NJ) on dry ice, and stored at -80 °C until EPR measurement was performed. The EPR spectra were recorded using Bruker X-band spectrometer (BRUKER, EMX-8/2.7, UCL, Brussels, Belgium) equipped with a Varian TE102 and a Varian temperature controller. Samples were maintained at -125 °C during the recording of signal. Parameters used for low temperature Fe (III) EPR were as follows: central field, 1520 G; sweep width, 500 G; resolution, 1024 points; frequency, 9.44 GHz; microwave power, 20.067 mW; receiver gain, 4.48e+4; conversion, 81.920 ms; time constant, 81.920 ms; sweep time, 83.886 s; number of scan, 4. EPR data was processed using Bruker WinEPR program.

### Acknowledgments

This work was supported by a grant from the National Basic Research Program of China (2004CB19604), a grant from the National Hi-Tech Development Program (2007AA021305), a key project from the National Natural Science Foundation of China (30830006), the project "Application of Nuclear Techniques in Agriculture" from the Chinese Ministry of Agriculture (200803034) and a project from Science and Technology Department of Zhejiang Province of China (2006E10058) to YJH.

### Appendix A. Supplementary data

Supplementary data associated with this article can be found, in the online version, at doi:10.1016/j.ygeno.2009.08.001.

## References

- [1] R.R. Khakhar, J.A. Cobb, L. Bjergbaek, I.D. Hickson, S.M. Gasser, RecQ helicases: multiple roles in genome maintenance, *Trends Cell Biol.* 13 (2003) 493–501.
- [2] V. Morozov, A.R. Mushegian, E.V. Koonin, P. Bork, A putative nucleic acid-binding domain in Bloom's and Werner's syndrome helicases, *Trends Biochem. Sci.* 22 (1997) 417–418.
- [3] P.L. Opreko, W.H. Cheng, V.A. Bohr, Junction of RecQ helicase biochemistry and human disease, *J. Biol. Chem.* 279 (2004) 18099–18102.
- [4] M. Muftuoglu, R. Kusumoto, E. Speina, G. Beck, W.H. Cheng, V.A. Bohr, Acetylation regulates WRN catalytic activities and affects base excision DNA repair, *PLoS ONE* 3 (2008) e1918.
- [5] P. Mohaghegh, I.D. Hickson, DNA helicase deficiencies associated with cancer predisposition and premature ageing disorders, *Human Mol. Gen.* 10 (2001) 741.
- [6] C. Von Kobbe, A. May, C. Grandori, V.A. Bohr, Werner syndrome cells escape hydrogen peroxide-induced cell proliferation arrest, *FASEB J.* 18 (2004) 1970–1972.
- [7] C.Z. Bachrati, I.D. Hickson, RecQ helicases: suppressors of tumorigenesis and premature aging, *Biochem. J.* 374 (2003) 577–606.
- [8] J.A. Cobb, L. Bjergbaek, S.M. Gasser, RecQ helicases: at the heart of genetic stability, *FEBS Lett.* 529 (2002) 43–48.
- [9] R.C. Fry, T.G. Sambandan, C. Rha, DNA damage and stress transcripts in *Saccharomyces cerevisiae* mutant sgs1, *Mech. Ageing Dev.* 124 (2003) 839–846.
- [10] K.S. Makarova, L. Aravind, Y.I. Wolf, R.L. Tatusov, K.W. Minton, E.V. Koonin, M.J. Daly, Genome of the extremely radiation-resistant bacterium *Deinococcus radiodurans* viewed from the perspective of comparative genomics, *Microbiol. Mol. Biol. Rev.* 65 (2001) 44–79.
- [11] M.P. Killoran, J.L. Keck, Three HRDC domains differentially modulate *Deinococcus radiodurans* RecQ DNA helicase biochemical activity, *J. Biol. Chem.* 281 (2006) 12849–12857.
- [12] L.F. Huang, X.T. Hua, H.M. Lu, G.J. Gao, B. Tian, B.H. Shen, Y.J. Hua, Functional analysis of helicase and three tandem HRDC domains of RecQ in *Deinococcus radiodurans*, *J. Zhejiang Univ. Sci. B* 7 (2006) 373–376.
- [13] L. Huang, X. Hua, H. Lu, G. Gao, B. Tian, B. Shen, Y. Hua, Three tandem HRDC domains have synergistic effect on the RecQ functions in *Deinococcus radiodurans*, *DNA Repair (Amst)* 6 (2007) 167–176.
- [14] L.F. Huang, S.W. Zhang, X.T. Hua, G.J. Gao, Y.J. Hua, Construction of the recQ double mutants and analysis of adversity in *Deinococcus radiodurans*, *Wei Sheng Wu Xue Bao* 46 (2006) 205–209.
- [15] X. Qiu, M.J. Daly, A. Vasilenko, M.V. Omelchenko, E.K. Gaidamakova, L. Wu, J. Zhou, G.W. Sundin, J.M. Tiedje, Transcriptome analysis applied to survival of *Shewanella oneidensis* MR-1 exposed to ionizing radiation, *J. Bacteriol.* 188 (2006) 1199–1204.
- [16] H. Chen, G. Xu, Y. Zhao, B. Tian, H. Lu, X. Yu, Z. Xu, N. Ying, S. Hu, Y. Hua, A Novel OxyR Sensor and Regulator of Hydrogen Peroxide Stress with One Cysteine Residue in *Deinococcus radiodurans*, *PLoS ONE* 3 (2008) e1602.
- [17] J. Boyd, M.N. Oza, J.R. Murphy, Molecular cloning and DNA sequence analysis of a diphtheria toxin iron-dependent regulatory element (dtxR) from *Corynebacterium diphtheriae*, *Proc. Natl. Acad. Sci. U. S. A.* 87 (1990) 5968–5972.
- [18] A. Glasfeld, E. Guedon, J.D. Helmann, R.G. Brennan, Structure of the manganese-bound manganese transport regulator of *Bacillus subtilis*, *Nat. Struct. Biol.* 10 (2003) 652–657.
- [19] M. Tanaka, A.M. Earl, H.A. Howell, M.J. Park, J.A. Eisen, S.N. Peterson, J.R. Battista, Analysis of *Deinococcus radiodurans*'s transcriptional response to ionizing radiation and desiccation reveals novel proteins that contribute to extreme radioresistance, *Genetics* 168 (2004) 21–33.
- [20] S.C. Andrews, A.K. Robinson, F. Rodriguez-Quinones, Bacterial iron homeostasis, *FEMS Microbiol. Rev.* 27 (2003) 215–237.
- [21] O. White, J.A. Eisen, J.F. Heidelberg, E.K. Hickey, J.D. Peterson, R.J. Dodson, D.H. Haft, M.L. Gwinn, W.C. Nelson, D.L. Richardson, K.S. Moffat, H. Qin, L. Jiang, W. Pamphile, M. Crosby, M. Shen, J.J. Vamathevan, P. Lam, L. McDonald, T. Utterback, C. Zalewski, K.S. Makarova, L. Aravind, M.J. Daly, K.W. Minton, R.D. Fleischmann, K.A. Ketchum, K.E. Nelson, S. Salzberg, H.O. Smith, J.C. Venter, C.M. Fraser, Genome sequence of the radioresistant bacterium *Deinococcus radiodurans* R1, *Science* 286 (1999) 1571–1577.
- [22] C. Ratledge, L.G. Dover, Iron metabolism in pathogenic bacteria, *Annu. Rev. Microbiol.* 54 (2000) 881–941.
- [23] Y. Liu, J. Zhou, M.V. Omelchenko, A.S. Beliaev, A. Venkateswaran, J. Stair, L. Wu, D.K. Thompson, D. Xu, I.B. Rogozin, E.K. Gaidamakova, M. Zhai, K.S. Makarova, E.V. Koonin, M.J. Daly, Transcriptome dynamics of *Deinococcus radiodurans* recovering from ionizing radiation, *Proc. Natl. Acad. Sci. U. S. A.* 100 (2003) 4191–4196.
- [24] H. Chen, Z.J. Xu, B. Tian, W.W. Chen, S.N. Hu, Y.J. Hua, Transcriptional profile in response to ionizing radiation at low dose in *Deinococcus radiodurans*, *Progress in Natural Science* 17 (2007) 525–536.
- [25] D. Ghosal, M.V. Omelchenko, E.K. Gaidamakova, V.Y. Matrosova, A. Vasilenko, A. Venkateswaran, M. Zhai, H.M. Kostandarithes, H. Brim, K.S. Makarova, L.P. Wackett, J.K. Fredrickson, M.J. Daly, How radiation kills cells: survival of *Deinococcus radiodurans* and *Shewanella oneidensis* under oxidative stress, *FEMS Microbiol. Rev.* 29 (2005) 361–375.
- [26] L.C. Seaver, J.A. Imlay, Are respiratory enzymes the primary sources of intracellular hydrogen peroxide? *J. Biol. Chem.* 279 (2004) 48742–48750.
- [27] J.A. Imlay, Cellular defenses against superoxide and hydrogen peroxide, *Annu. Rev. Biochem.* (2008).
- [28] L.M. Markillie, S.M. Varnum, P. Hradecky, K.K. Wong, Targeted mutagenesis by duplication insertion in the radioresistant bacterium *Deinococcus radiodurans*: radiation sensitivities of catalase (katA) and superoxide dismutase (sodA) mutants, *J. Bacteriol.* 181 (1999) 666–669.
- [29] S.G. Kim, G. Bhattacharyya, A. Grove, Y.H. Lee, Crystal structure of Dps-1, a functionally distinct Dps protein from *Deinococcus radiodurans*, *J. Mol. Biol.* 361 (2006) 105–114.
- [30] M.G. Cuypers, E.P. Mitchell, C.V. Romao, S.M. McSweeney, The crystal structure of the Dps2 from *Deinococcus radiodurans* reveals an unusual pore profile with a non-specific metal binding site, *J. Mol. Biol.* 371 (2007) 787–799.
- [31] M.J. Daly, E.K. Gaidamakova, V.Y. Matrosova, A. Vasilenko, M. Zhai, A. Venkateswaran, M. Hess, M.V. Omelchenko, H.M. Kostandarithes, K.S. Makarova, L.P. Wackett, J.K. Fredrickson, D. Ghosal, Accumulation of Mn(II) in *Deinococcus radiodurans* facilitates gamma-radiation resistance, *Science* 306 (2004) 1025–1028.
- [32] W. Gao, Y. Liu, C.S. Giometti, S.L. Tollaksen, T. Khare, L. Wu, D.M. Klingeman, M.W. Fields, J. Zhou, Knock-out of SO1377 gene, which encodes the member of a conserved hypothetical bacterial protein family COG2268, results in alteration of iron metabolism, increased spontaneous mutation and hydrogen peroxide sensitivity in *Shewanella oneidensis* MR-1, *BMC Genomics* 7 (2006) 76.
- [33] J.F. Ma, U.A. Ochsner, M.G. Klotz, V.K. Nanayakkara, M.L. Howell, Z. Johnson, J.E. Posey, M.L. Vasil, J.J. Monaco, D.J. Hassett, Bacterioferritin A modulates catalase A (KatA) activity and resistance to hydrogen peroxide in *Pseudomonas aeruginosa*, *J. Bacteriol.* 181 (1999) 3730–3742.
- [34] J.C. Crack, J. Green, N.E. Le Brun, A.J. Thomson, Detection of sulfide release from the oxygen-sensing [4Fe-4S] cluster of FNR, *J. Biol. Chem.* 281 (2006) 18909–18913.
- [35] N.S. Jakubovics, H.F. Jenkinson, Out of the iron age: new insights into the critical role of manganese homeostasis in bacteria, *Microbiology* 147 (2001) 1709–1718.
- [36] M.J. Daly, E.K. Gaidamakova, V.Y. Matrosova, A. Vasilenko, M. Zhai, R.D. Leapman, B. Lai, B. Ravel, S.M. Li, K.M. Kemner, J.K. Fredrickson, Protein oxidation implicated as the primary determinant of bacterial radioresistance, *PLoS Biol.* 5 (2007) e92.
- [37] V. Mattimore, K.S. Udupa, G.A. Berne, J.R. Battista, Genetic characterization of forty ionizing radiation-sensitive strains of *Deinococcus radiodurans*: linkage information from transformation, *J. Bacteriol.* 177 (1995) 5232–5237.
- [38] D. Xu, G. Li, L. Wu, J. Zhou, Y. Xu, PRIMEGENS: robust and efficient design of gene-specific probes for microarray analysis, *Bioinformatics* 18 (2002) 1432–1437.
- [39] G.K. Smyth, Limma: linear models for microarray data, in: R. Gentleman, V. Carey, S. Dudoit, R. Irizarry, W. Huber (Eds.), *Bioinformatics and Computational Biology Solutions Using R and Bioconductor*, Springer, New York, 2005, pp. 397–420.
- [40] Y.H. Yang, S. Dudoit, P. Luu, D.M. Lin, V. Peng, J. Ngai, T.P. Speed, Normalization for cDNA microarray data: a robust composite method addressing single and multiple slide systematic variation, *Nucleic Acids Res.* 30 (2002) e15.
- [41] G.K. Smyth, J. Michaud, H.S. Scott, Use of within-array replicate spots for assessing differential expression in microarray experiments, *Bioinformatics* 21 (2005) 2067–2075.
- [42] K.Z. Gong, Z.G. Zhang, A.H. Li, Y.F. Huang, P. Bu, F. Dong, J. Liu, ROS-mediated ERK activation in delayed protection from anoxic preconditioning in neonatal rat cardiomyocytes, *Chin. Med. J. (Engl.)* 117 (2004) 395–400.
- [43] K. Keyer, J.A. Imlay, Superoxide accelerates DNA damage by elevating free-iron levels, *Proc. Natl. Acad. Sci. U. S. A.* 93 (1996) 13635–13640.